THE JOURNAL OF BIOLOGICAL CHEMISTRY VOL. 289, NO. 35, pp. 24304–24313, August 29, 2014

Valosin-containing Protein-interacting Membrane Protein (VIMP) Links the Endoplasmic Reticulum with Microtubules in Concert with Cytoskeleton-linking Membrane Protein (CLIMP)-63*

Received for publication, April 4, 2014, and in revised form, July 1, 2014 Published, JBC Papers in Press, July 9, 2014, DOI 10.1074/jbc.M114.571372

Chikano Noda[‡1], Hana Kimura[‡1], Kohei Arasaki[‡1], Mitsuru Matsushita[‡], Akitsugu Yamamoto[§], Yuichi Wakana[‡], Hiroki Inoue[‡], and Mitsuo Tagaya[‡2]

From the [‡]Department of Molecular Life Sciences, School of Life Sciences, Tokyo University of Pharmacy and Life Sciences, Hachioji, Tokyo 192-0392 and the [§]Faculty of Bioscience, Nagahama Institute of Bio-Science and Technology, Nagahama, Shiga 526-0829, Japan

Background: The distribution and morphology of the mammalian endoplasmic reticulum (ER) are regulated by microtubules (MTs).
Results: Valosin-containing protein (VCP)-interacting membrane protein (VIMP) interacts with both MTs and the rough ER-localized cytoskeleton-linking membrane protein (CLIMP)-63. Its overexpression or depletion affects ER structure.
Conclusion: VIMP links the ER and MTs.
Significance: VIMP not only recruits VCP to the ER but also regulates ER shape.

The distribution and morphology of the endoplasmic reticulum (ER) in mammalian cells depend on both dynamic and static interactions of ER membrane proteins with microtubules (MTs). Cytoskeleton-linking membrane protein (CLIMP)-63 is exclusively localized in sheet-like ER membranes, typical structures of the rough ER, and plays a pivotal role in the static interaction with MTs. Our previous study showed that the 42-kDa ER-residing form of syntaxin 5 (Syn5L) regulates ER structure through the interactions with both CLIMP-63 and MTs. Here, we extend our previous study and show that the valosin-containing protein/p97-interacting membrane protein (VIMP)/SelS is also a member of the family of proteins that shape the ER by interacting with MTs. Depletion of VIMP causes the spreading of the ER to the cell periphery and affects an MT-dependent process on the ER. Although VIMP can interact with CLIMP-63 and Syn5L, it does not interact with MT-binding ER proteins (such as Reep1) that shape the tubular smooth ER, suggesting that different sets of MT-binding ER proteins are used to organize different ER subdomains.

The endoplasmic reticulum (ER)[3] is a continuous membrane system but consists of a variety of subdomains that are responsible for executing diverse functions of the ER, such as protein synthesis and export, lipid synthesis, calcium homeostasis, and protein degradation (which is known as ER-associated degradation) (1). Morphologically, the ER structure can be classified into two general groups: tubular and sheet-like structures that represent typical smooth and rough ER membrane structures, respectively (2–5).

Microtubules (MTs) play important roles in the organization and dynamics of ER membranes in mammalian cells via their dynamic and static interactions with ER-residing proteins (6). For example, ER membranes bind to the growing tips of MTs through an ER membrane protein, STIM1, and an MT plus end-binding protein, EB1 (7, 8). ER tubules bind to the shaft of an existing MT and slide along MTs (8, 9), in particular, on curved acetylated MTs (10). Sliding is driven by MT motors, kinesin and cytoplasmic dynein (11, 12). The static interaction between ER membranes and MTs is mediated by several ER-residing proteins (6).

We recently reported that the 42-kDa form of syntaxin 5 (Syn5L), which is generated by alternative initiation of translation and resides in the ER as well as the Golgi apparatus (13), contributes to the organization of the ER structure by interacting with both cytoskeleton-linking membrane protein (CLIMP)-63/CKAP4 and MTs (14). CLIMP-63 is localized exclusively in the rough ER and mediates a static interaction with MTs (15–17). Overexpression of Syn5L, as well as that of CLIMP-63 (15), induces rearrangement and co-alignment of the ER membrane with MTs (14). This ER-MT bundling has been reported to be induced by overexpression of several MT-binding ER proteins (6, 18, 19), including Reep1 (20). Reep1, a member of the DP1/Yop1 superfamily, is predominantly local-

* This work was supported in part by Grants-in-aid for Scientific Research 24657141 and 25291029 (to M. T.) from the Ministry of Education, Culture, Sports, Science and Technology of Japan.
[1] These authors contributed equally to this work.
[2] To whom correspondence should be addressed: Department of Molecular Life Sciences, School of Life Sciences, Tokyo University of Pharmacy and Life Sciences, 1432-1 Horinouchi, Hachioji, Tokyo 192-0392, Japan. Tel.: 81-42-676-5419; Fax: 81-42-676-5468; E-mail: tagaya@toyaku.ac.jp.
[3] The abbreviations used are: ER, endoplasmic reticulum; MT, microtubule; Syn, syntaxin; CLIMP, cytoskeleton-linking membrane protein; RTN, reticulon; ATL, atlastin; VCP, valosin-containing protein; VIMP, VCP/p97-interacting membrane protein; BFA, brefeldin A; mRFP, monomeric red fluorescent protein; PFA, paraformaldehyde; VSVG, vesicular stomatitis virus-encoded glycoprotein.

ized in tubular smooth ER membranes (20). The DP1/Yop1, reticulon (RTN), and atlastin (ATL) families of proteins (6, 21, 22) and the MT-severing protein spastin (23) interact with one another and coordinate MT interactions with the tubular ER network (20).

Valosin-containing protein (VCP)-interacting membrane protein (VIMP) was discovered as an ER-localized VCP/p97-interacting protein (24) and is alternatively called SelS because of its possession of selenocysteine at the penultimate amino acid residue (25). The previous finding that overexpressed VIMP exhibits filamentous structures including ER membrane proteins (24) encouraged us to explore whether this protein, like CLIMP-63 (15) and Syn5L (14), regulates ER structure by interacting with MTs and MT-binding proteins. In this study, we show that VIMP interacts with MTs and the rough ER protein CLIMP-63, but not with the smooth ER proteins, and regulates ER structure.

EXPERIMENTAL PROCEDURES

Antibodies and Reagents—Bacterially expressed GST-VIMP lacking the transmembrane domain was purified using glutathione beads and injected to rabbits. The antibody was affinity-purified using Sepharose 4B (GE Healthcare) coupled with His_6-tagged VIMP lacking the transmembrane domain. A polyclonal anti-Bap31 antibody was prepared as reported previously (26). A monoclonal antibody against CLIMP-63 was obtained from Enzo Life Science. Monoclonal antibodies against GM130 and calnexin were obtained from Pharmingen. Monoclonal and polyclonal antibodies against FLAG and α-tubulin were obtained from Sigma-Aldrich. An antiserum against Sec61β was purchased from Millipore Corp. A goat anti-RTN4 antibody and a rabbit anti-GST antibody were purchased from Santa Cruz Biotechnology. A polyclonal anti-VCP antibody was from Thermo Fisher Scientific. Brefeldin A (BFA), nocodazole, and Taxol were from Sigma-Aldrich.

Cell Culture—293T cells were grown in Dulbecco's modified Eagle's medium supplemented with 50 IU/ml penicillin, 50 μg/ml streptomycin, and 10% fetal calf serum. HeLa cells were cultured in Eagle's minimum essential medium supplemented with the same materials. HeLa cells stably expressing monomeric red fluorescent protein (mRFP)-Sec61β were established previously (14).

Plasmids and Transfection—The cDNAs encoding VIMP and its truncation mutants were inserted into pFLAG-CMV-6c (Sigma-Aldrich). Construction of a Syn5L mutant and RTN family proteins was as reported previously (14, 27). The cDNA encoding VIMP(48–187) was inserted into pGEX-4T-3. The cDNAs encoding Reep1/Reep5 and ATL1 (gifts from Dr. Craig Blackstone, NINDS, Bethesda, MD) were inserted into pFLAG-CMV-5a and pFLAG-CMV-6c, respectively, so as to express Reep1 and Reep5 each with a C-terminal FLAG tag and ATL1 with an N-terminal FLAG tag.

Immunoprecipitation—Immunoprecipitation was performed as described previously (14). For immunoprecipitation of endogenous VIMP, 293T cells were homogenized in homogenization buffer (20 mM Hepes-KOH (pH 7.2), 150 mM KCl, 2 mM EDTA, 1 mM dithiothreitol, 10 μg/ml leupeptin, 1 μM pepstatin A, 2 μg/ml aprotinin, and 1 mM phenylmethylsulfonyl fluoride), and the membrane pellet was solubilized in homogenization buffer containing 1% Triton X-100. For immunoprecipitation of expressed proteins, 293T cells expressing FLAG-tagged proteins were lysed in homogenization buffer containing 1% Triton X-100.

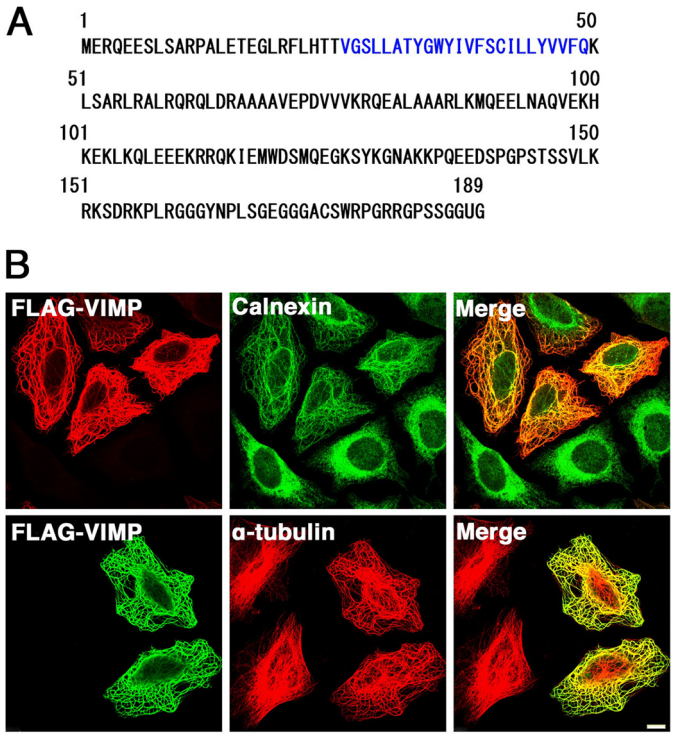

FIGURE 1. **Overexpression of FLAG-VIMP causes ER-MT bundling.** *A*, amino acid sequence of VIMP. Amino acid residues in the putative transmembrane domain are shown in *blue*. *U* represents the penultimate selenocysteine. *B*, at 24 h after transfection with the FLAG-VIMP(1–187) construct, HeLa cells were fixed and double-stained with antibodies against FLAG and calnexin (*upper panels*) or α-tubulin (*lower panels*). *Scale bar* = 5 μm.

Immunofluorescence Microscopy—For immunofluorescence microscopy, cells were fixed with 4% paraformaldehyde (PFA) for 20 min at room temperature and observed with an Olympus FluoView 300 or 1000 laser scanning microscope as described (28).

Immunoelectron Microscopy—Immunoelectron microscopy was performed as described previously (29), except that cells were fixed with 4% PFA for 30 min to retain immunoreactivity to VIMP.

Subcellular Fractionation—Subcellular fractionation was performed as described previously (30).

MT Sedimentation Assay—MT sedimentation assay was conducted as described previously (14) using porcine brain tubulin (Cytoskeleton, Inc.) After centrifugation, equal protein amounts of the supernatant and pellet fractions were subjected to SDS-PAGE and analyzed by immunoblotting with antibodies against GST and α-tubulin.

RNA Interference—The RNA duplexes used for targeting VIMP were VIMP(210) (5′-ggaaccugauguuguguuaa-3′), VIMP(247) (5′-gcagcugcucgacugaaaau-3′), CLIMP-63(748) (5′-gacaacaucgcc-aucuuca-3′), Syn18(390) (5-caggaccgcuguuuuggauuu-3), and Syn5(390) (5′-ggaaauugaagagcuaaca-3′). The number in parentheses after each protein name indicates the position of the first nucleotide of siRNA relative to the start codon. All siRNAs

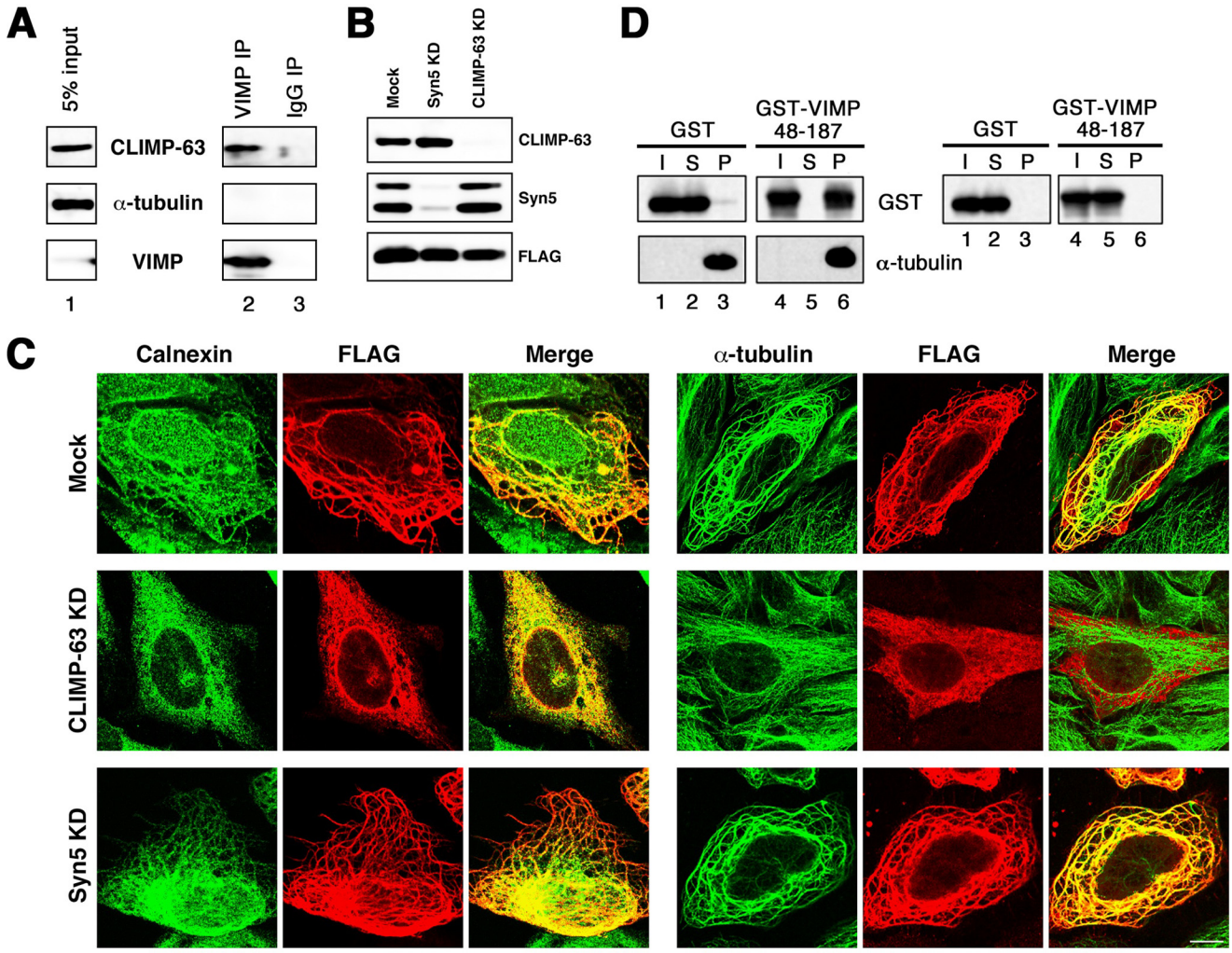

FIGURE 2. **VIMP interacts with both CLIMP-63 and polymerized MTs.** *A*, membrane fractions of 293T cell lysates were prepared, solubilized, and immunoprecipitated (*IP*) with an anti-VIMP antibody (*lane 2*) or a control IgG (*lane 3*). The precipitates were separated by SDS-PAGE and analyzed by immunoblotting with antibodies against CLIMP-63, α-tubulin, and VIMP. 5% of solubilized membranes was run as input (*lane 1*). *B* and *C*, HeLa cells were transfected without (*Mock*) or with siRNA targeting Syn5 or CLIMP-63. At 48 h after transfection, the cells were transfected with the plasmid for FLAG-VIMP(1–187). After 24 h, the cells were lysed, separated by SDS-PAGE, and analyzed by immunoblotting with the indicated antibodies (*B*). Alternatively, the cells were fixed and double-stained with antibodies against FLAG and calnexin (*C*, *left*) or α-tubulin (*right*). *KD*, knockdown. *Scale bar* = 10 μm. *D*, purified GST (*lanes 1–3*) and GST-VIMP(48–187) (*lanes 4–6*) were subjected to sedimentation with (*left*) or without (*right*) Taxol-stabilized MTs and analyzed by immunoblotting with the indicated antibodies. *I*, *S*, and *P* represent input, supernatant, and precipitate, respectively.

were purchased from Japan Bioservice. Transfection was performed using Oligofectamine (Invitrogen) according to the manufacturer's protocol.

Vesicular Stomatitis Virus-encoded Glycoprotein (VSVG)-GFP Transport Assay—The plasmid encoding ts045 VSVG-GFP was kindly supplied by Dr. Jennifer Lippincott-Schwartz (National Institutes of Health, Bethesda, MD). Assay was conducted as described previously (31).

RESULTS

Overexpression of VIMP Induces Rearrangement of the ER Network—VIMP is a 189-amino acid protein with one N-terminal transmembrane domain (amino acids 26–49) and luminal N-terminal and cytoplasmic C-terminal domains (Fig. 1*A*). A previous study showed that overexpression of VIMP altered ER morphology to filamentous structures (24). To examine whether MTs are involved in formation of the filamentous structure, we first overexpressed FLAG-VIMP(1–187) and compared the distribution of FLAG-VIMP-positive filaments with that of MTs. As shown in Fig. 1*B*, FLAG-VIMP caused the rearrangement of the ER, as seen by calnexin staining (*upper panels*), and MTs, as seen by α-tubulin staining (*lower panels*). This ER-MT-bundling pattern is almost the same as that observed in cells overexpressing CLIMP-63 (15) and Syn5L (14). A similar ER-MT-bundling pattern was observed in cells expressing FLAG-tagged full-length VIMP (amino acids 1–189) (data not shown).

Interaction of VIMP with CLIMP-63 and MTs—Given that VIMP has an ER-MT-bundling activity, we next examined whether it interacts with CLIMP-63. As shown in Fig. 2*A*, CLIMP-63 coprecipitated with an anti-VIMP antibody (*lane 2*), whereas no coprecipitation was observed with a control IgG (*lane 3*). Of note is that α-tubulin did not coprecipitate with VIMP, excluding the possibility that the link between VIMP and CLIMP-63 is mediated through tubulins. To assess the importance of the link between VIMP and CLIMP-63, we

knocked down CLIMP-63 by siRNA (Fig. 2*B*) and examined the formation of ER-MT bundling induced by VIMP overexpression. As shown in Fig. 2*C*, no clear bundling was detected in the absence of CLIMP-63 (*middle panels*), whereas bundling occurred in the absence of Syn5 (*lower panels*), which has been shown to bind to CLIMP-63 (14).

We then examined the interaction of VIMP with polymerized MTs. To this end, a VIMP construct (amino acids 48–187) lacking the transmembrane domain was expressed as a GST fusion protein in *Escherichia coli* and purified. The purified protein was mixed with Taxol-stabilized MTs and then subjected to sedimentation as described under "Experimental Procedures." As shown in Fig. 2*D*, almost all of GST-VIMP(48–187) (*left*, *lane 6*), but not GST (*lane 3*), coprecipitated with polymerized MTs. This coprecipitation did not occur in the absence of MTs (Fig. 2*D*, *right*, *lane 6*), suggesting the specific binding between VIMP and polymerized MTs.

The C-terminal Region of VIMP Is Important for the Interaction with CLIMP-63—To confirm the interaction between VIMP and CLIMP-63, we expressed VIMP as a FLAG-tagged protein in 293T cells and performed immunoprecipitation. As shown in Fig. 3*A* (*lane 12*), CLIMP-63 (*second panel*), in addition to VCP (*upper panel*) and the long form of Syn5 (Syn5L) (*third panel*), coprecipitated with FLAG-VIMP(1–187). A similar precipitation pattern was observed for FLAG-tagged full-length VIMP (data not shown), suggesting that selenocysteine is not involved in the interaction with these proteins. Because Syn5L coprecipitated with FLAG-VIMP, we examined the endogenous interaction between Syn5 and VIMP. We found little coprecipitation of Syn5 with an anti-VIMP antibody (data not shown), suggesting that the interaction of VIMP with Syn5L is weak compared with that with CLIMP-63.

To define the regions of VIMP responsible for the interactions with CLIMP-63 and Syn5, we produced a series of C-terminally truncated mutants. VIMP(1–175) showed a markedly decreased ability to bind to CLIMP-63, but retained Syn5L-binding ability (Fig. 3*A*, *lane 11*). VIMP(1–166) (*lane 10*), but not VIMP(1–146) (*lane 9*), was found to have Syn5L-binding activity. Essentially no binding to Syn5L or CLIMP-63 was observed for VIMP(1–73) (Fig. 3*A*, *lane 8*). The bundle-forming activity of VIMP appeared to be correlated with its CLIMP-63- and Syn5L-binding abilities. VIMP(1–175) and VIMP(1–166), both of which bound Syn5L but little or no CLIMP-63 (Fig. 3*A*, *lanes 10* and *11*), exhibited a bundling-staining pattern, but with a substantial background of diffuse staining (Fig. 3*B*, *second* and *third rows*). Bundling was not obvious for VIMP(1–146) (Fig. 3*B*, *fourth row*), which bound little or no CLIMP-63 or Syn5L (Fig. 3*A*, *lane 9*), and an ER- and/or plasma membrane-staining pattern was observed for VIMP(1–73) (Fig. 3*B*, *lower row*).

Intuitively, the data in Fig. 3*B* (*second* and *third rows*) appear to be contradictory to the finding that CLIMP-63 is essential for ER-MT bundling (Fig. 2*C*). The VIMP constructs with very low CLIMP-63-binding activities could induce ER-MT bundling. This can be reconciled with the idea that CLIMP-63 is a principal ER-MT anchor protein, whereas VIMP and Syn5L are secondary ones. In the pres-

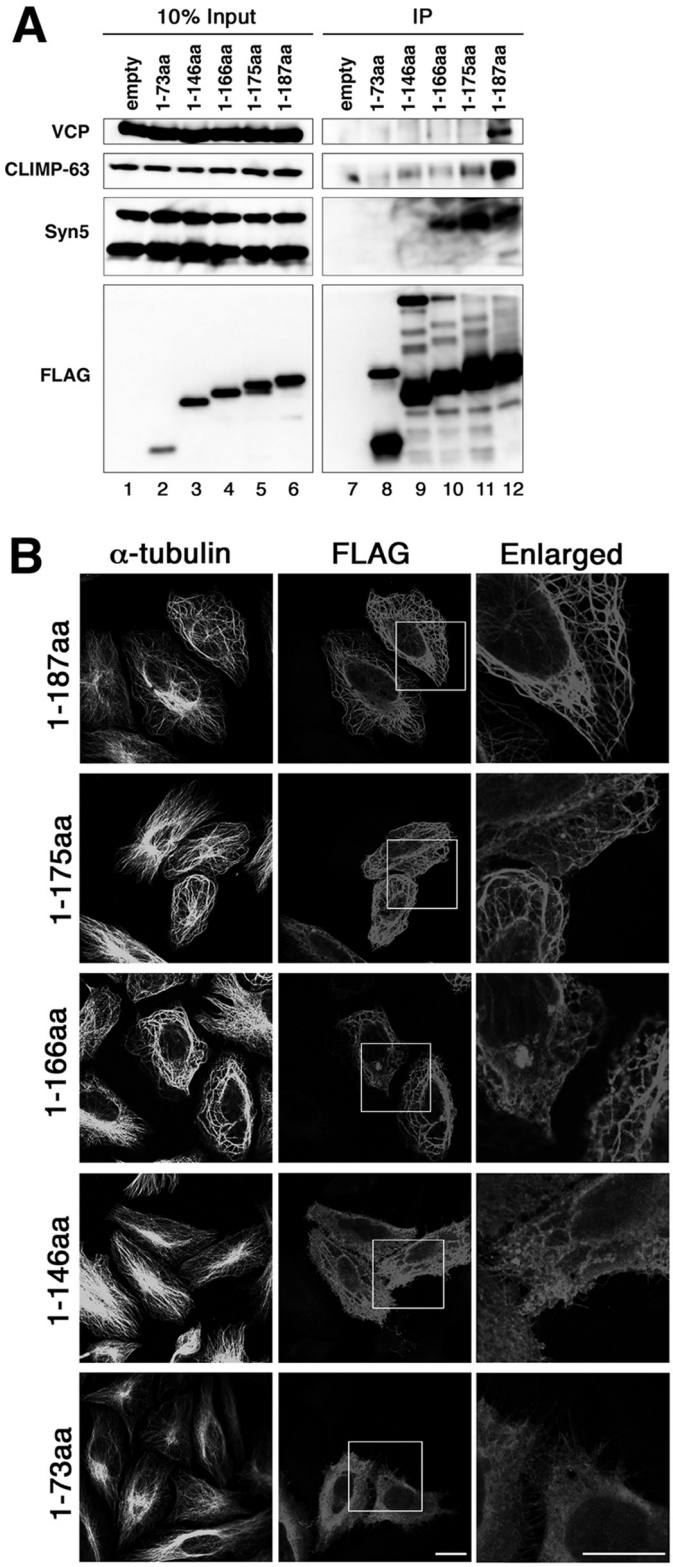

FIGURE 3. **The C-terminal region of VIMP is important for binding to CLIMP-63.** *A*, at 24 h after transfection of 293T cells with the indicated FLAG-VIMP constructs, cell lysates were prepared, immunoprecipitated (*IP*) with anti-FLAG M2 beads, and immunoblotted with the indicated antibodies. *B*, at 24 h after transfection with the indicated FLAG-VIMP constructs, HeLa cells were fixed and double-stained with antibodies against α-tubulin and FLAG. The *boxed areas* are enlarged on the *right*. *Scale bars* = 10 μm. *aa*, amino acids.

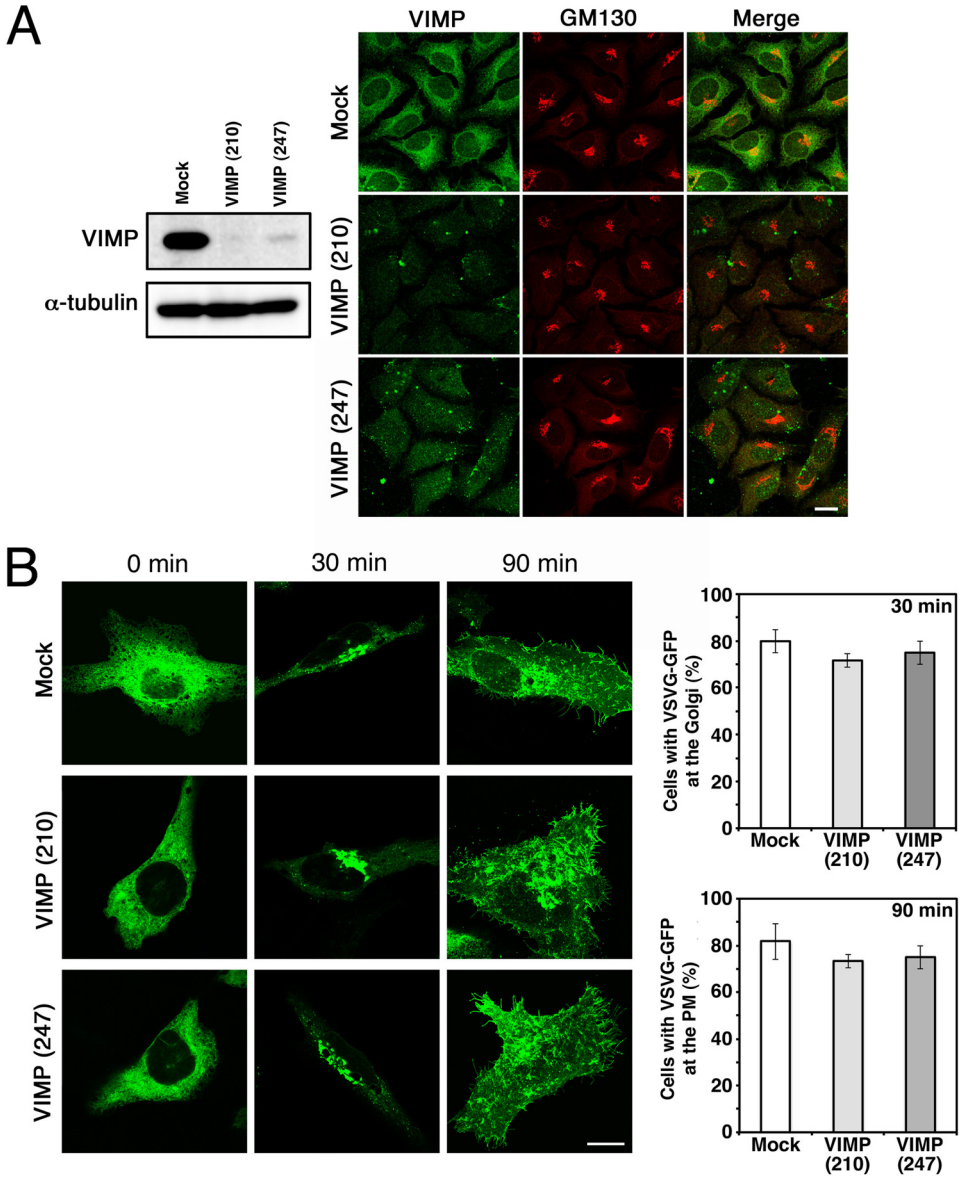

FIGURE 4. **Knockdown of VIMP does not significantly affect protein transport from the ER.** HeLa cells were transfected without (*Mock*) or with one of the siRNAs targeting VIMP (siRNA(210) or siRNA(247)). *A*, after 72 h, the cells were analyzed by immunoblotting (*left*) or double-stained with antibodies against VIMP and a Golgi marker, GM130 (*right*). *Scale bar* = 10 μm. *B*, alternatively, at 48 h after transfection, the cells were transfected with the plasmid encoding VSVG-GFP and incubated for an additional 24 h. VSVG-GFP transport from the ER to the plasma membrane (*PM*) through the Golgi was analyzed by immunofluorescence microscopy. *Scale bar* = 10 μm. Quantitative data represent the average of three independent experiments, with S.D. indicated by *error bars*. In each experiment, 30 cells were analyzed.

ence of endogenous CLIMP-63, the ER is fully attached to MTs; therefore, the interaction of overexpressed VIMP with endogenous Syn5L might be enough to form ER-MT bundles (Fig. 3*B*, *second* and *third rows*). In contrast, in the absence of CLIMP-63, the association of overexpressed VIMP with endogenous Syn5L might be insufficient for the formation of ER-MT bundles (Fig. 2*C*).

Depletion of VIMP Causes Spreading of the ER—To investigate whether VIMP is involved in the organization of the ER, we knocked down VIMP expression and examined the morphology of the ER. Both siRNA(210) and siRNA(247) effectively knocked down VIMP expression (Fig. 4*A*). Of note, no dispersal of a Golgi marker (GM130) was observed, suggesting that ER-to-Golgi transport is not impaired in VIMP-depleted cells. Consistent with this idea, the transport of VSVG-GFP from the ER to the plasma membrane through the Golgi apparatus was not significantly affected by VIMP depletion (Fig. 4*B*). In contrast, both siRNAs caused spreading of the ER membrane proteins Sec61β and CLIMP-63 to the cell periphery (Fig. 5*A*). These spreading patterns were similar to those in cells depleted of CLIMP-63 or Syn5 (14), suggesting the involvement of VIMP in shaping the ER.

In cells depleted of Syn5, the distribution of spread ER membranes was not affected by the MT-depolymerizing reagent nocodazole (14). To show that depletion of VIMP specifically affects ER structure, not cell shape, we treated mRFP-Sec61β-expressing cells with nocodazole and performed live cell imaging. As shown in Fig. 5*B*, nocodazole treatment of VIMP-depleted cells did not cause further mRFP-Sec61β spreading, whereas the centrally accumulated mRFP-Sec61β in mock-

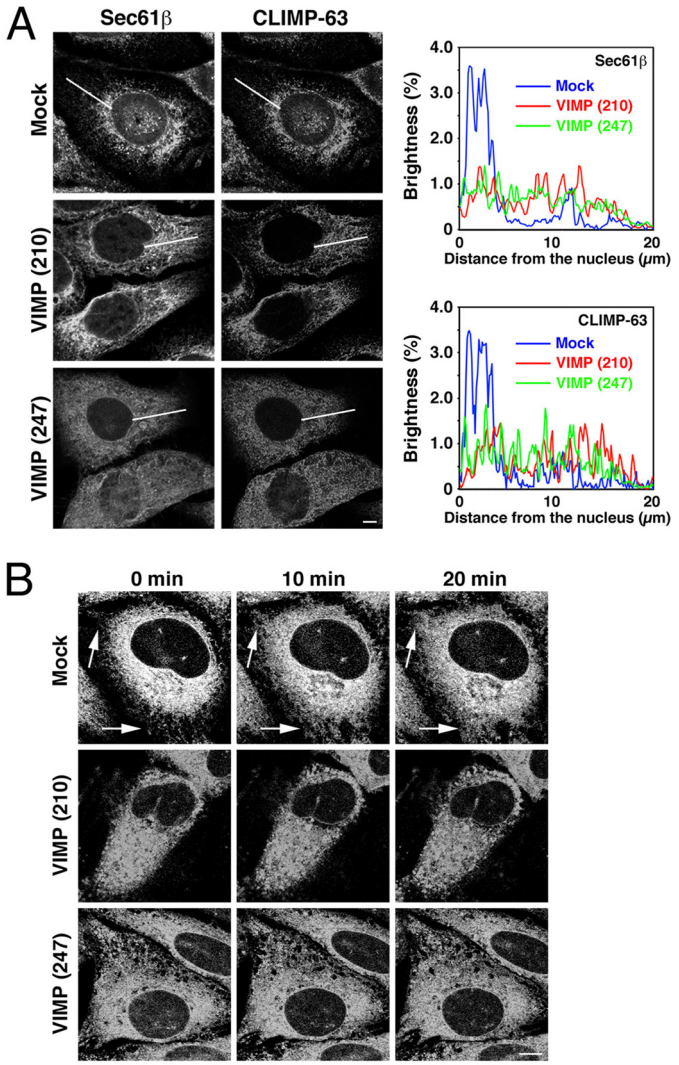

FIGURE 5. **Knockdown of VIMP causes ER spreading.** HeLa cells (*A*) or those stably expressing mRFP-Sec61β (*B*) were transfected without (*Mock*) or with one of the siRNAs targeting VIMP (siRNA(210) or siRNA(247)). *A*, after 72 h, the HeLa cells were fixed and stained with an antibody against Sec61β (*left*) or CLIMP-63 (*right*). Sec61β or CLIMP-63 fluorescence along *white lines* from the nucleus to the cell periphery was analyzed using ImageJ software. The average values of fluorescence brightness in five cells are shown. *Scale bar* = 5 μm. *B*, alternatively, HeLa cells stably expressing mRFP-Sec61β were incubated with 5 μg/ml nocodazole, and live cell imaging was performed. Representative images at the indicated times are shown. *Arrows* indicate peripheral regions, where ER structures were rarely seen before nocodazole treatment. *Scale bar* = 5 μm.

treated cells was redistributed to more peripheral regions upon nocodazole treatment.

VIMP Affects an MT-dependent Process on the ER Membrane—Our previous study showed that an ER membrane protein, Bap31, undergoes one-time cycling between the peripheral and perinuclear ER regions in an MT-dependent manner after treatment with BFA, an inhibitor of the ARF1 (ADP-ribosylation factor 1) guanine nucleotide exchange factor (32), followed by its washout (26). This may reflect the fact that the movement of Bap31 to the perinuclear region within the ER is ARF1-dependent (26). To explore the link between VIMP and an MT-dependent process, we investigated the effect of VIMP depletion on the cycling of Bap31 within the ER. In mock-treated cells, BFA treatment/washout caused the movement of Bap31 to the perinuclear region at 120–240 min after BFA washout (Fig. 6, *left*), and the accumulated Bap31 returned to the cell periphery by 360 min in a considerable fraction of cells (*lower row*). In contrast, in VIMP-depleted cells, Bap31 exhibited large punctate peripheral staining at 120 min after BFA washout and did not accumulate at the perinuclear region (Fig. 6, *right*). At 360 min after BFA washout, Bap31 remained as punctuate structures in many cells (Fig. 6, *lower row*). These results suggest that the MT- and dynein-dependent movement of Bap31 to the perinuclear region is inhibited by VIMP depletion.

VIMP Does Not Interact with Tubular ER-shaping Proteins—Our previous study showed that Lys-82 of Syn5L is important for binding to CLIMP-63 and MTs (14). As shown in Fig. 7*A*, this residue is also responsible for the interaction with VIMP.

Next, we examined whether VIMP interacts with proteins (such as the RTN, DP1/Yop1, and ATL families) that are responsible for shaping the smooth ER (20, 21, 33). These protein families and the MT-severing protein spastin interact with one another and coordinate MT interactions with the tubular ER network (20). As shown in Fig. 7 (*B* and *C*), Reep family members (Reep1 and Reep5 each represent two distinct Reep1 subfamilies (20)), ATL1, RTN3, RTN4a, RTN4b, and RTN4c were found not to bind to FLAG-VIMP.

VIMP Is Excluded from Smooth ER Aggregates in Syn18-depleted Cells—To determine the distribution of VIMP in the ER, we first performed subcellular fractionation using a 5–25% OptiPrep gradient. In our protocol, VIMP almost completely co-sedimented with CLIMP-63 with a peak in fractions 6 and 7, whereas the smooth ER marker RTN4 sedimented in fractions 4–9 without a clear peak (Fig. 8*A*). Next, we sought to examine the distribution of VIMP by immunoelectron microscopy. Because the immunoreactivity of our antibody to VIMP was lost upon fixation of cells with 4% PFA plus 0.1% glutaraldehyde for 30 min or with 4% PFA for 2 h, we observed cells fixed with 4% PFA for 30 min. Because of mild fixation, the ultrastructure was slightly obscure, but the presence of VIMP on ER membranes was seen (Fig. 8*B*, *arrows*).

As we could not clearly demonstrate the presence of VIMP on the rough ER, we examined whether VIMP behaves like rough ER membrane proteins upon Syn18 depletion. Our previous work showed that knockdown of Syn18, a SNARE localized in the ER (34), causes segregation of rough and smooth ER membranes (29), although the precise mechanism underlying this phenomenon remains unclear. In Syn18-depleted cells, smooth ER membrane proteins such as RTN4 aggregate to form patch-like structures, whereas rough ER membrane proteins such as CLIMP-63 and Sec61β remain largely unchanged and are almost completely excluded from the patch-like structures (29). We knocked down Syn18 and stained cells with antibodies against VIMP and smooth or rough ER markers. In mock-treated cells, the distribution of all proteins examined was almost indistinguishable at the level of immunofluorescence microscopy (Fig. 9, *A* and *B*, *left*). As reported previously (29), in Syn18-depleted cells, RTN4 became aggregated, whereas CLIMP-63 and Sec61β largely retained their distributions except for the absence in RTN4-positive patches (Fig. 9*A*, *right*). Similarly, VIMP did not accumulate at the aggregates

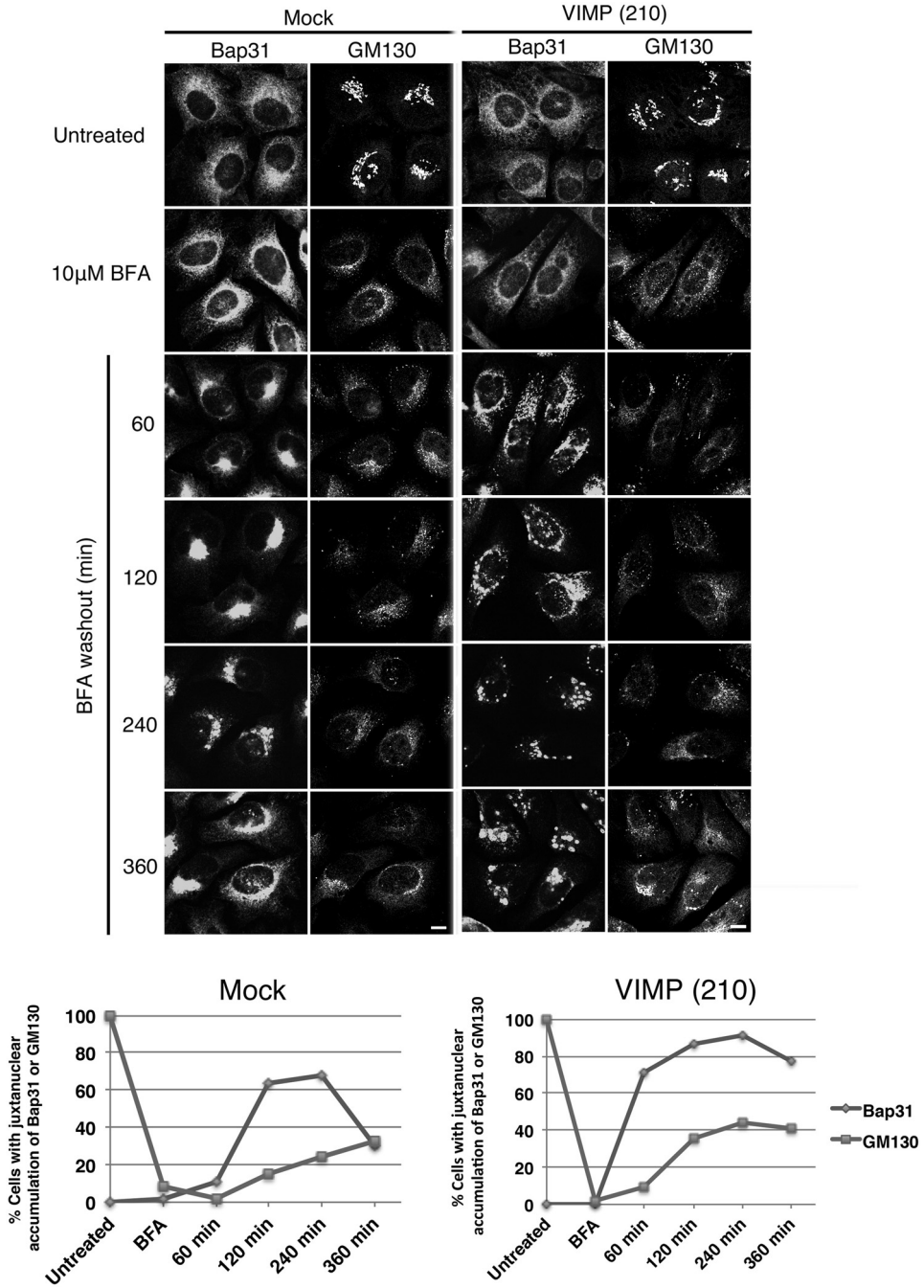

FIGURE 6. **Knockdown of VIMP affects the cycling of Bap31 within the ER after BFA washout.** HeLa cells were transfected without (*Mock*) or with siRNA(210). At 66 h after transfection, BFA was added to a final concentration of 10 μM, and the cells were incubated for 30 min and then washed to remove BFA. At the indicated times after BFA washout, the cells were fixed and double-stained with antibodies against Bap31 and GM130. *Scale bar* = 5 μm. Quantitative data are shown at the bottom. Experiments were repeated three times with similar results.

and largely retained normal morphology (Fig. 9*B*, *right*), consistent with the finding that VIMP specifically interacts with rough ER membrane proteins.

DISCUSSION

MTs play an important role in the organization of the ER in mammalian cells. The static interaction between ER membranes and MTs is mediated by several ER-residing proteins (6). We have recently demonstrated that the ER-residing form of Syn5 (Syn5L) regulates ER structure by interacting with both CLIMP-63 and MTs (14). In the present study, we have shown that VIMP also contributes to the organization of the ER by interacting with both CLIMP-63 and MTs. It should be noted that VIMP binds to polymerized MTs (Fig. 2*D*), but not depolymerized tubulin (Fig. 2*A*), suggesting that VIMP directly interacts with CLIMP-63, not through tubulin.

As in the case of Syn5L (14), ER-MT bundle formation induced by VIMP overexpression is dependent on the presence of CLIMP-63. Mutation analysis revealed a rough correlation between bundle formation and abilities to interact with

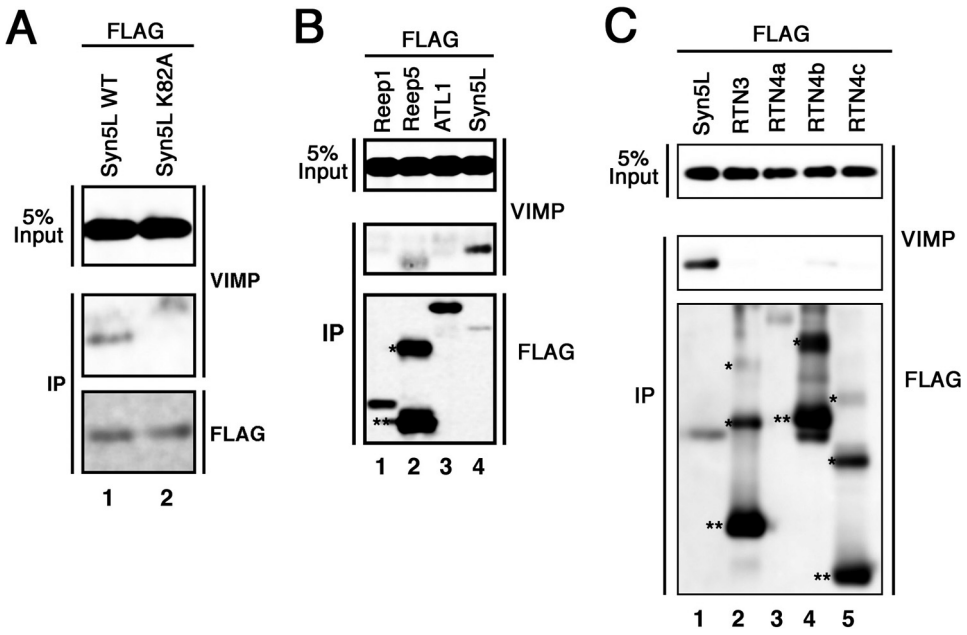

FIGURE 7. **VIMP does not interact with smooth ER-shaping proteins.** Lysates of 293T cells expressing FLAG-tagged wild-type Syn5L or mutant K82A (*A*); Reep1-FLAG, Reep5-FLAG, FLAG-ATL1, or FLAG-tagged wild-type Syn5L (*B*); or FLAG-tagged wild-type Syn5L or one of the FLAG-RTN proteins (*C*) were subjected to immunoprecipitation (*IP*) with anti-FLAG M2 beads and analyzed by immunoblotting with antibodies against VIMP and FLAG. Oligomer (*) and monomer (**) species are indicated.

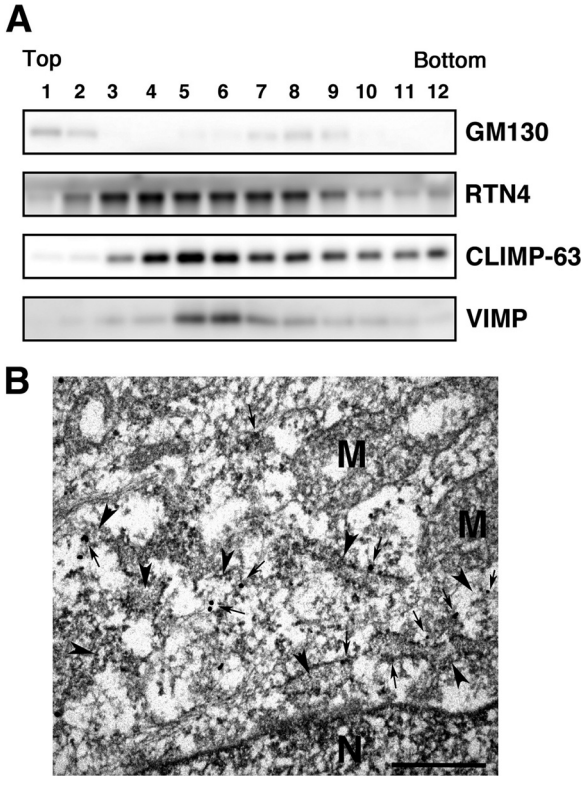

FIGURE 8. **Localization of VIMP.** *A*, lysates of HeLa cells were subjected to fractionation using a 5–25% OptiPrep gradient. Fractions (0.3 ml each) were collected from the top of the gradient. Appropriate portions of each fraction were subjected to SDS-PAGE and analyzed by immunoblotting with antibodies against Golgi marker GM130 (*upper panel*), RTN4 (*second panel*), CLIMP-63 (*third panel*), and VIMP (*lower panel*). *B*, immunoelectron micrograph. *Arrowheads* and *arrows* indicate ER membranes and immunoreactivity to VIMP, respectively. *N* and *M* denote nucleus and mitochondria, respectively. *Scale bar* = 0.5 μm.

CLIMP-63 and Syn5L. Of note, Lys-82 of Syn5L is responsible for the interaction with VIMP as well as with CLIMP-63 and MTs (14). Perhaps multivalent and cooperative interactions of VIMP with MT-binding proteins and MTs are necessary for ER-MT bundle formation. It should be emphasized that CLIMP-63 serves as a critical hub for MT-binding ER proteins.

Depletion of VIMP caused spreading of the ER membrane, a characteristic phenotype observed when the link between the ER and MTs is disrupted by nocodazole treatment (14, 35). A difference in the effects of nocodazole treatment and VIMP depletion is that the Golgi apparatus is disassembled by MT depolymerization, whereas no Golgi disassembly is induced by VIMP depletion. In addition to a morphological change in the ER, VIMP depletion affected one round of MT-dependent Bap31 cycling after BFA washout. These results suggest that VIMP is involved in MT-dependent processes on the ER, but not in other pathways such as ER-to-Golgi transport and the maintenance of the steady-state distribution of GM130.

Like CLIMP-63 (21), VIMP was found not to interact with smooth ER-shaping proteins. Moreover, our data show that VIMP did not accumulate in smooth ER patches in Syn18-depleted cells, although we could not clearly demonstrate that VIMP is localized in rough ER membranes by immunoelectron microscopy. Blackstone and co-workers (20) suggested the possibility that Reep1 and CLIMP-63 play similar roles in mediating ER-MT interactions in different ER subdomains. Extending their idea, we have hypothesized that multivalent and cooperative interactions between ER membrane proteins, such as CLIMP-63 (15, 16), Syn5L (14), Syn5-interacting proteins (polycystins (36)), and those between

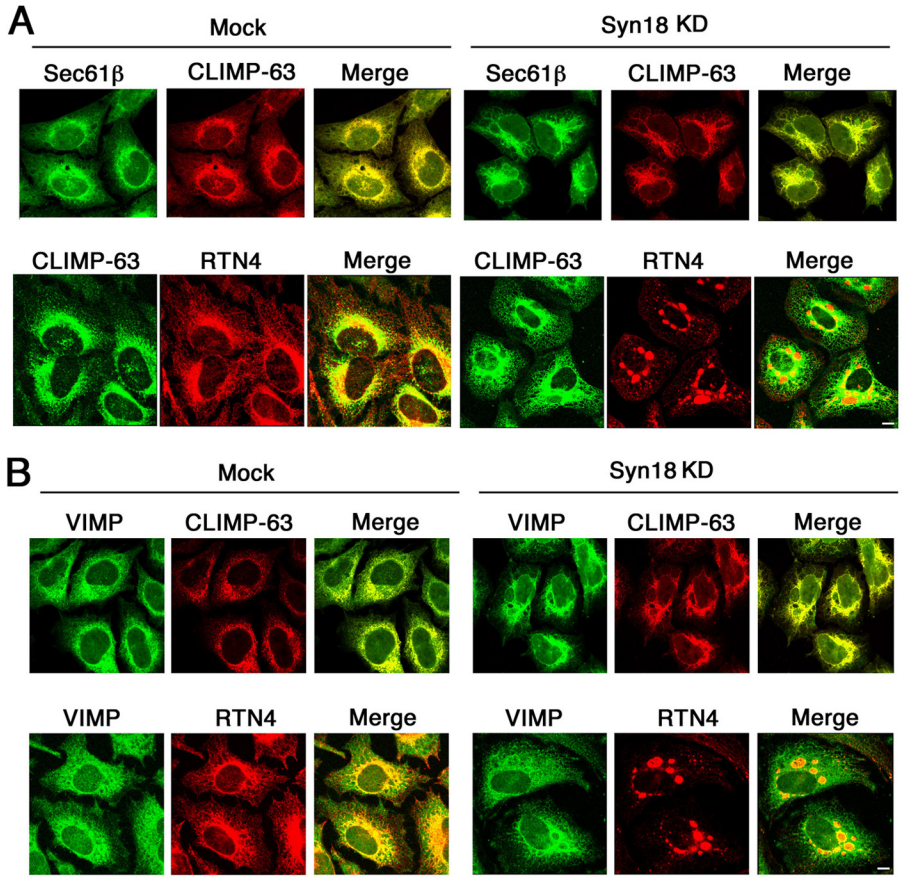

FIGURE 9. **Depletion of Syn18 does not induce redistribution of VIMP.** HeLa cells were transfected without (*Mock*) or with siRNA targeting Syn18 (siRNA(390)). After 72 h, the cells were fixed and double-stained with antibodies against CLIMP-63 and Sec61β (*A*, *upper panels*) or RTN4 (*A*, *lower panels*) or VIMP and CLIMP-63 (*B*, *upper panels*) or RTN4 (*B*, *lower panels*). *Scale bars* = 10 μm. *KD*, knockdown.

these proteins and MTs are required for the organization of the rough ER (14). Our present results reveal that VIMP is such an ER-shaping protein.

Acknowledgments—We thank Naohiko Hirota and Yuki Konno for technical assistance and Drs. Craig Blackstone and Jennifer Lippincott-Schwartz for kind gifts of plasmids.

REFERENCES

1. Lynes, E. M., and Simmen, T. (2011) Urban planning of the endoplasmic reticulum (ER): how diverse mechanisms segregate the many functions of the ER. *Biochim. Biophys. Acta* **1813,** 1893–1905
2. Shibata, Y., Hu, J., Kozlov, M. M., and Rapoport, T. A. (2009) Mechanisms shaping the membranes of cellular organelles. *Annu. Rev. Cell Dev. Biol.* **25,** 329–354
3. Friedman, J. R., and Voeltz, G. K. (2011) The ER in 3D: a multifunctional dynamic membrane network. *Trends Cell Biol.* **21,** 709–717
4. Chen, S., Novick, P., and Ferro-Novick, S. (2013) ER structure and function. *Curr. Opin. Cell Biol.* **25,** 428–433
5. Goyal, U., and Blackstone, C. (2013) Untangling the web: mechanisms underlying ER network formation. *Biochim. Biophys. Acta* **1833,** 2492–2498
6. Vedrenne, C., and Hauri, H.-P. (2006) Morphogenesis of the endoplasmic reticulum: beyond active membrane expansion. *Traffic* **7,** 639–646
7. Grigoriev, I., Gouveia, S. M., van der Vaart, B., Demmers, J., Smyth, J. T., Honnappa, S., Splinter, D., Steinmetz, M. O., Putney, J. W., Jr., Hoogenraad, C. C., and Akhmanova, A. (2008) STIM1 is a MT-plus-end-tracking protein involved in remodeling of the ER. *Curr. Biol.* **18,** 177–182
8. Waterman-Storer, C. M., and Salmon, E. D. (1998) Endoplasmic reticulum membrane tubules are distributed by microtubules in living cells using three distinct mechanisms. *Curr. Biol.* **8,** 798–806
9. Lee, C., Ferguson, M., and Chen, L. B. (1989) Construction of the endoplasmic reticulum. *J. Cell Biol.* **109,** 2045–2055
10. Friedman, J. R., Webster, B. M., Mastronarde, D. N., Verhey, K. J., and Voeltz, G. K. (2010) ER sliding dynamics and ER-mitochondrial contacts occur on acetylated microtubules. *J. Cell Biol.* **190,** 363–375
11. Woźniak, M. J., and Allan, V. J. (2006) Cargo selection by specific kinesin light chain 1 isoforms. *EMBO J.* **25,** 5457–5468
12. Woźniak, M. J., Bola, B., Brownhill, K., Yang, Y. C., Levakova, V., and Allan, V. J. (2009) Role of kinesin-1 and cytoplasmic dynein in endoplasmic reticulum movement in VERO cells. *J. Cell Sci.* **122,** 1979–1989
13. Hui, N., Nakamura, N., Sönnichsen, B., Shima, D. T., Nilsson, T., and Warren, G. (1997) An isoform of the Golgi t-SNARE, syntaxin 5, with an endoplasmic reticulum retrieval signal. *Mol. Biol. Cell* **8,** 1777–1787
14. Miyazaki, K., Wakana, Y., Noda, C., Arasaki, K., Furuno, A., and Tagaya, M. (2012) Contribution of the long form of syntaxin 5 to the organization of the endoplasmic reticulum. *J. Cell Sci.* **125,** 5658–5666
15. Klopfenstein, D. R., Kappeler, F., and Hauri, H.-P. (1998) A novel direct interaction of endoplasmic reticulum with microtubules. *EMBO J.* **17,** 6168–6177
16. Klopfenstein, D. R., Klumperman, J., Lustig, A., Kammerer, R. A., Oorschot, V., and Hauri, H.-P. (2001) Subdomain-specific localization of CLIMP-63 (p63) in the endoplasmic reticulum is mediated by its luminal α-helical segment. *J. Cell Biol.* **153,** 1287–1300
17. Shibata, Y., Shemesh, T., Prinz, W. A., Palazzo, A. F., Kozlov, M. M., and Rapoport, T. A. (2010) Mechanisms determining the morphology of the peripheral ER. *Cell* **143,** 774–788
18. Gao, H., Sellin, L. K., Pütz, M., Nickel, C., Imgrund, M., Gerke, P., Nitschke, R., Walz, G., and Kramer-Zucker, A. G. (2009) A short carboxy-terminal domain of polycystin-1 reorganizes the microtubular network

and the endoplasmic reticulum. *Exp. Cell Res.* **315,** 1157–1170
19. Ogawa-Goto, K., Tanaka, K., Ueno, T., Tanaka, K., Kurata, T., Sata, T., and Irie, S. (2007) p180 is involved in the interaction between the endoplasmic reticulum and microtubules through a novel microtubule-binding and bundling domain. *Mol. Biol. Cell* **18,** 3741–3751
20. Park, S. H., Zhu, P. P., Parker, R. L., and Blackstone, C. (2010) Hereditary spastic paraplegia proteins REEP1, spastin, and atlastin-1 coordinate microtubule interactions with the tubular ER network. *J. Clin. Invest.* **120,** 1097–1110
21. Hu, J., Shibata, Y., Zhu, P. P., Voss, C., Rismanchi, N., Prinz, W. A., Rapoport, T. A., and Blackstone, C. (2009) A class of dynamin-like GTPases involved in the generation of the tubular ER network. *Cell* **138,** 549–561
22. Orso, G., Pendin, D., Liu, S., Tosetto, J., Moss, T. J., Faust, J. E., Micaroni, M., Egorova, A., Martinuzzi, A., McNew, J. A., and Daga, A. (2009) Homotypic fusion of ER membranes requires the dynamin-like GTPase atlastin. *Nature* **460,** 978–983
23. Errico, A., Ballabio, A., and Rugarli, E. I. (2002) Spastin, the protein mutated in autosomal dominant hereditary spastic paraplegia, is involved in microtubule dynamics. *Hum. Mol. Genet.* **11,** 153–163
24. Ye, Y., Shibata, Y., Yun, C., Ron, D., and Rapoport, T. A. (2004) A membrane protein complex mediates retro-translocation from the ER lumen into the cytosol. *Nature* **429,** 841–847
25. Shchedrina, V. A., Zhang, Y., Labunskyy, V. M., Hatfield, D. L., and Gladyshev, V. N. (2010) Structure-function relations, physiological roles, and evolution of mammalian ER-resident selenoproteins. *Antioxid. Redox Signal.* **12,** 839–849
26. Wakana, Y., Takai, S., Nakajima, K., Tani, K., Yamamoto, A., Watson, P., Stephens, D. J., Hauri, H.-P., and Tagaya, M. (2008) Bap31 is an itinerant protein that moves between the peripheral endoplasmic reticulum (ER) and a juxtanuclear compartment related to ER-associated degradation. *Mol. Biol. Cell* **19,** 1825–1836
27. Wakana, Y., Koyama, S., Nakajima, K., Hatsuzawa, K., Nagahama, M., Tani, K., Hauri, H.-P., Melançon, P., and Tagaya, M. (2005) Reticulon 3 is involved in membrane trafficking between the endoplasmic reticulum and Golgi. *Biochem. Biophys. Res. Commun.* **334,** 1198–1205
28. Tagaya, M., Furuno, A., and Mizushima, S. (1996) SNAP prevents Mg^{2+}-ATP-induced release of *N*-ethylmaleimide-sensitive factor from the Golgi apparatus in digitonin-permeabilized PC12 cells. *J. Biol. Chem.* **271,** 466–470
29. Iinuma, T., Aoki, T., Arasaki, K., Hirose, H., Yamamoto, A., Samata, R., Hauri, H.-P., Arimitsu, N., Tagaya, M., and Tani, K. (2009) Role of syntaxin 18 in the organization of endoplasmic reticulum subdomains. *J. Cell Sci.* **122,** 1680–1690
30. Gilady, S. Y., Bui, M., Lynes, E. M., Benson, M. D., Watts, R., Vance, J. E., and Simmen, T. (2010) Ero1α requires oxidizing and normoxic conditions to localize to the mitochondria-associated membrane (MAM). *Cell Stress Chaperones* **15,** 619–629
31. Presley, J. F., Cole, N. B., Schroer, T. A., Hirschberg, K., Zaal, K. J., and Lippincott-Schwartz, J. (1997) ER-to-Golgi transport visualized in living cells. *Nature* **389,** 81–85
32. Donaldson, J. G., Finazzi, D., and Klausner, R. D. (1992) Brefeldin A inhibits Golgi membrane-catalysed exchange of guanine nucleotide onto ARF protein. *Nature* **360,** 350–352
33. Voeltz, G. K., Prinz, W. A., Shibata, Y., Rist, J. M., and Rapoport, T. A. (2006) A class of membrane proteins shaping the tubular endoplasmic reticulum. *Cell* **124,** 573–586
34. Hatsuzawa, K., Hirose, H., Tani, K., Yamamoto, A., Scheller, R. H., and Tagaya, M. (2000) Syntaxin 18, a SNAP receptor that functions in the endoplasmic reticulum, intermediate compartment, and *cis*-Golgi vesicle trafficking. *J. Biol. Chem.* **275,** 13713–13720
35. Lu, L., Ladinsky, M. S., and Kirchhausen, T. (2009) Cisternal organization of the endoplasmic reticulum during mitosis. *Mol. Biol. Cell* **20,** 3471–3480
36. Geng, L., Boehmerle, W., Maeda, Y., Okuhara, D. Y., Tian, X., Yu, Z., Choe, C. U., Anyatonwu, G. I., Ehrlich, B. E., and Somlo, S. (2008) Syntaxin 5 regulates the endoplasmic reticulum channel-release properties of polycystin-2. *Proc. Natl. Acad. Sci. U.S.A.* **105,** 15920–15925